ADVANCED SYNTHESIS OF CARBON DOTS
Novel Insights into Temperature Effect on Fluorescent Performance

by

Shen SHEN[a,b], Jia-Jia FU[a,b,c*], Hong-Bo WANG[a,b*], and Wei-Dong GAO[a,b]

[a] Jiangsu Engineering Technology Research Center for Functional Textiles, Jiangnan University, Wuxi, China
[b] Key Laboratory of Eco-Textiles, Ministry of Education, Jiangnan University, Wuxi, China
[c] Jiangsu Sunshine Group Co., Ltd., Sunshine Industrial Park, Xinqiao Town, Jiangyin, China

Original scientific paper
https://doi.org/10.2298/TSCI1904453S

As a new generation of semiconductor reinforcements, fluorescent carbon dots have unpredictable and potential applications in bioimaging, photocatalysis, and optoelectronic devices. This work shows an environmentally friendly process for carbon dots preparation using citric acid monohydrate and urea. The influence of different parameters on luminous property was carefully studied based on the photoluminescence intensity measurement, including synthesis temperature, time and the concentration of carbon sources and deactivator. Then the synthesized products were further characterized by TEM, FT-IR, XPS, UV-vis, and XRD. Highest fluorescence intensity could be achieved under the carbon sources and deactivator concentration of 0.3 mol/L and 1 mol/L, respectively, in a total reaction system of 40 ml at 190 °C for 18 hours. The screening analysis revealed that synthesis temperature has a strong correlation with the photoluminescence intensity. This study provides further insights into designing high fluorescent performance for carbon dots preparation.

Key words: *fluorescent carbon dots, synthesis temperature, UV-vis absorption, photoluminescence intensity*

Introduction

Luminescent nanomaterials have been used in wide range of fields, including gene transmission, drug carriers, bioimaging probes, chemical sensors, and analytical chemistry [1]. Fluorescent nanoparticles, known as the famous luminescent nanomaterials, have evoked intense interest in recent decades owning to the emergence of new fluorescent nanoparticles, such as semiconductor quantum dots, graphene dots, carbon dots (CD), *etc*. [1-3] Carbon is one of the abundant elements in the universe with various allotropes. Carbon-based nanomaterials, (*i. e.* graphene, fullerenes, nanodiamonds, carbon nanotubes, CD, *etc.*) have large specific surface area and *plentiful* surface traps. In particular, CD are one of burgeoning fluorescent nanomaterials, constituting a class of nanosized particle which generally refers to photoluminescence (PL) carbon nanoparticles less than 10 nm in size [4, 5]. Such materials are undoubtedly accepted as a promising candidate for a variety of applications. Typically, they have sp^2 and sp^3 hybridized carbon-layer structures and can keep oxygen in the form of various oxygen-containing species, such as hydroxyl (–OH), carboxyl (–COOH), and aldehyde

* Corresponding author, e-mail: kathyfjj@126.com, wxwanghb@163.com

(–CHO) functional groups, on their surface, thus imparting them with good water solubility, excellent biocompatibility, high conductivity, photochemical stability, and suitability for subsequent fabrication with various organic, polymeric, inorganic or biological species [6, 7].

The unique properties and surface structures of CD mainly depend on the preparation methods and precursors used for synthesis. Therefore, the preparation with appropriate carbon precursors and methods is the key issue, which should be considered to improve their properties [8]. Hydrothermal method, known as hydrothermal carbonization, is regarded as the irreplaceable and efficient technique for forming the CD. Its main reaction principle is to take use of high temperature and pressure to overcome the limitations of raw materials and drawbacks of undesirable yield. In addition, compared with traditional preparing approaches, hydrothermal method is friendly to the environment and can lead to the surface functionalization by introducing functional groups, significantly enhancing the stability and biocompatibility of formed CD [6, 9].

Experimental

Materials and reagents

Citric acid monohydrate and urea were supplied by Sinopharm Chemical Reagent Co., Ltd, China (SCRC). High-purity water from ULUPURE pure ultrapure water/water system was used throughout the experiments. All other chemicals were of analytical pure grad.

Preparation of CD

In this paper, citric acid monohydrate/urea as precursors were co-carbonized to synthesize highly bright CD via a facile green route of hydrothermal method. In a typical process, certain concentration of citric acid monohydrate and urea were dissolved in 40 mL high-purity water. After stirring, the mixture was transferred into a Teflon-lined stainless steel autoclave and maintained at a constant temperature for several hours. Then the solution was naturally cooled down and centrifuged at 12000 rpm for 20 minute to eliminate the residues. Finally, the supernatant was stored at –4 °C for further use. A single factor experiment was employed for a better understanding of the processing parameters effect on the PL intensity of CD, including temperature, time, the concentration of citric acid monohydrate and urea. Table 1 presents the factors and their levels of single factor experiment.

Table 1. Factors and their levels of single factor experiment

Levels	Citric acid monohydrate [molL^{-1}]	Urea [molL^{-1}]	Reaction time [hours]	Reaction temperature [°C]
1	0.075	0.25	5	160
2	0.15	0.50	8	170
3	0.225	0. 75	12	180
4	0.3	1.0	18	190
5	0.375	1.25	22	200

Characterization of CD

Fourier transform infrared spectra (FTIR) was accomplished by Thermo Nicolet IS10 spectrometer in the scan range of 4000-500 cm^{-1} using KBr pellet method. Fluorescence

spectra of liquid sample was performed by FS5 Spectrafluorometer (EDINBURGH INSTRUMENTS) at room temperature. The UV-visible absorption spectra was recorded on Thermo multiskan GO in the wavelength range from 250 nm to 700 nm. The crystal structure was identified by a Brukey SMART APEXII X-ray diffractometer (XRD) using Cu Kα radiation with a scanning rate of 5° per minute in the range from 10° to 80°. The surface composition and chemical states were analyzed by X-ray photoelectron spectroscopy（XPS）using Thermo ESCALAB 250XI with a base vacuum operated at 300 W. High-resolution transmission electron microscopy (HRTEM) measurement was carried out on a HITACHI H-8100 electron microscopy (Hitachi, Tokyo, Japan) with an accelerating voltage of 200 kV to characterize their morphology and distribution.

Results and discussion

Optimum parameters for CD preparation

The proper synthesis temperature, the time, the concentration of citric acid and urea are the key factors in the synthesis of qualified fluorescence CD.

Synthesis temperature predominantly determines the formation status, the carbonization degree and the PL behavior of CD. Figure 1(a) presented PL intensity of CD achieved by using various synthesis temperature (160-200 °C) while maintaining other synthesis parameters the same. As can be seen in fig. 1(a), less CD were formed at lower temperature in synthesis process at the initial stage, since low synthesis temperature may lead to slow formation rate of CD and carbon core, which in turn affected their PL intensity [10, 11]. When the synthesis temperature reached 190 °C, a stronger intense PL spectrum appeared due to the dehydration of citric acid-urea. If the synthesis temperature were controlled below 190 °C, an enhancement trend of PL intensity would be observed. CD surface groups, *i. e.*, *pyridine* derivatives, are intrinsically relaying on the *solvent* and can form H-bonding interactions. Therefore, surface groups are susceptible to establish the relations through intermolecular H bonds [12]. Moreover, such intermolecular H-bonds are more sensitive to temperature than the intramolecular H-bonds. Under higher thermolysis temperature, the intermolecular H-bonds between NH groups and water molecules become weakened, leading to the slow burning of the surface-bounded N (amide) and the creation of intramolecular H-bonds. Further, the hydrothermal temperature play a vital role in controlling the surface passivation with heteroatoms and generating intramolecular H-bonds with fluorophores (in different structures) and surface groups [12, 13].

Figure 1(b) displayed the dependence of PL intensity of CD on the concentration of urea. The PL intensity increased linearly with the concentration of urea in the range from 0.25 mol/L to 1 mol/L. However, the curve exhibited deteriorating trend when the concentration of urea reached 1.25 mol/L. The highest PL intensity was obtained under the urea concentration of 1 mol/L. This exception can be explained that a higher concentration of urea might provoke the increase of modified $-NH_2$ group (primary radiative PL centers) and the decrease of oxygenated functional groups (non-radiative PL centers). Subsequently, the PL intensity of CD with different reaction time was presented in fig 1(c). The increase of reaction time appreciably affected the fluorescent property, which might accelerate the nanoparticles formation. However, such trend was not compatible with the PL intensity at 22 hour since the overlong reaction time might cause excessive carbonation and result in the reduction of oxygenated functional groups, thus lead to a lower PL intensity.

The concentration of citric acid plays a key role in synthesis process. Figure 1(d) presented the PL intensity of CD in response to the concentration of citric acid under the fixed condition (temperature: 190 °C, urea: 1.0 mol/L, time: 18 hours). In the certain concentration scope, higher citric acid concentration led to greater PL intensity. On the contrary, lower PL intensity was observed when the citric acid concentration reached 0.375 mol/L, which might be attributed to the re-absorption of CD at the superfluous citric acid solution [13].

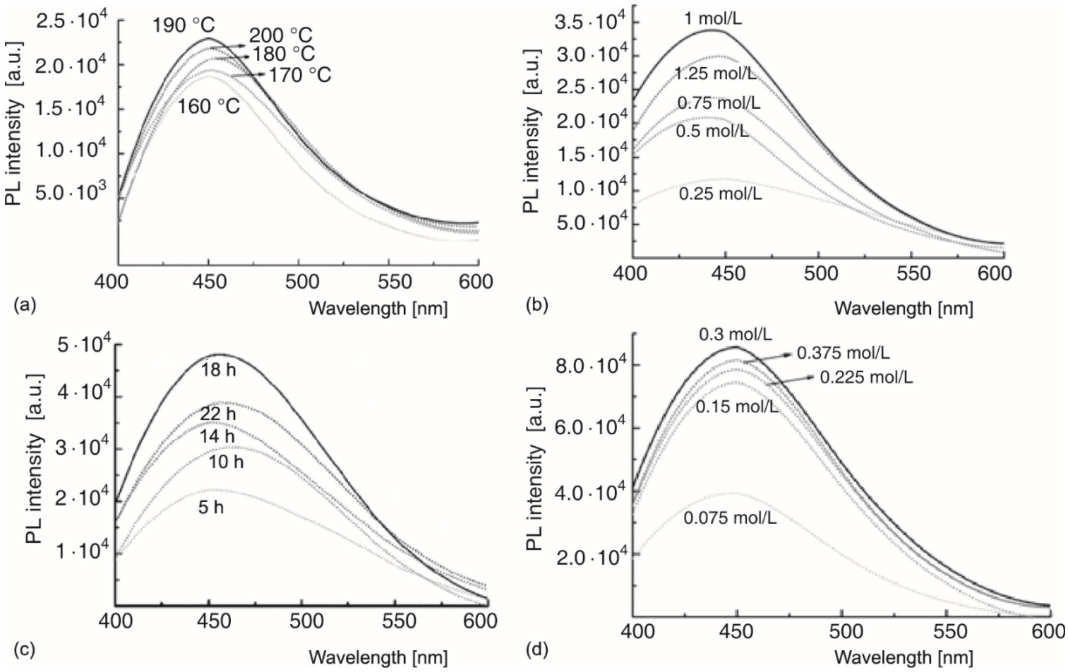

Figure 1. The PL intensity of CD with different parameters; (a) synthesis temperature, (b) concentration of urea, (c) reaction time, and (d) concentration of citric acid

Property of CD

As shown in fig. 2, FT-IR spectra of CD exhibited an extremely broad band at the range from 3100 cm^{-1} to 3500 cm^{-1} corresponding to the stretching vibrations of O-H and N-H. Besides, the vibration peaks of C=O (1640 cm^{-1}), C=C (1580 cm^{-1}), C–N= (1410 cm^{-1}) can also be observed, suggesting the presence of large number of hydroxyl groups, carboxylic and amino groups on the on the surface of CD, which made CD be convenient to couple with other groups and therefore can greatly extend their application in the future.

The CD generally have a strong absorption under the UV light. The typical UV-vis absorption spectra and PL spectra are portrayed in fig. 3. The CD displayed a broad absorption in the range 250-300 nm with a reduced intensity absorption extending into the visible light region. The absorption spectrum showed a peak at around 270-300 nm, which was mainly ascribed to the $\pi \rightarrow \pi^*$ transition of C=O. The absorption from 300 nm to 400 nm may arise from n-π^* transition of surface C=O and C=N bonds, respectively. Meanwhile, the CD gave rise to high photoluminescence with a maximum value at 475 nm by excitation at UV light.

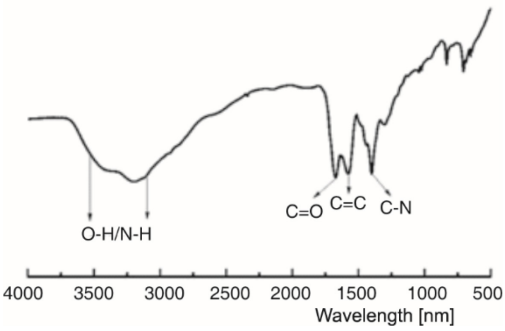

Figure 2. The FTIR spectra of CD

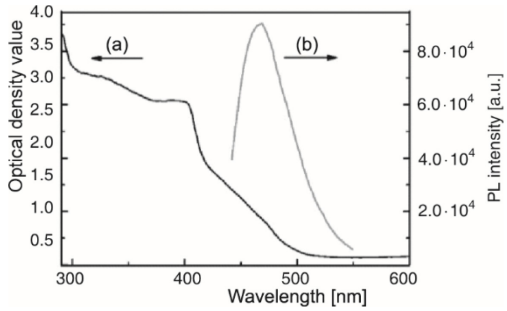

Figure 3. The UV-Vis absorption and PL emission spectra of CD; (a) absorption spectra of CD, (b) emission spectra of CD

The XPS was conducted to further delve the chemical bonds and functional groups of synthesized CD (as shown in fig. 4). Figure 4(a) presented the high resolution C1s spectrum of, where the binding energy peaks centered at 284.5 eV, 285.3 eV, 286.2 eV, 288,2 eV can be attributed to sp^2 and sp^3 carbons (C=C/C-C), sp^3 carbons (C-N) and (C-O), carbonyl carbons (C=O) [14]. In the high resolution N1s spectrum, fig. 4(b), the binding energies of C-N-C and N-H were located at 399.6 eV and 401.1 eV, respectively. The high resolution O1s, fig. 4(c), fitted into two main peaks at 531.3 eV, 532.8 eV, were corresponding to C=O and C-O [15].

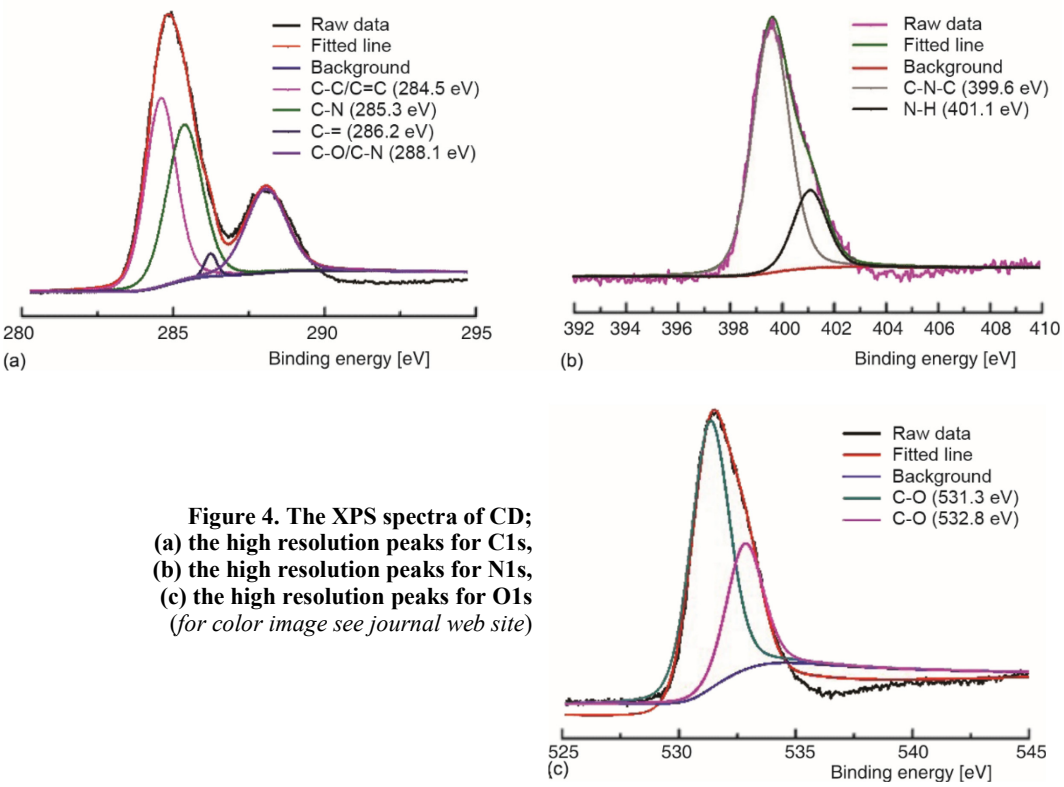

Figure 4. The XPS spectra of CD; (a) the high resolution peaks for C1s, (b) the high resolution peaks for N1s, (c) the high resolution peaks for O1s (*for color image see journal web site*)

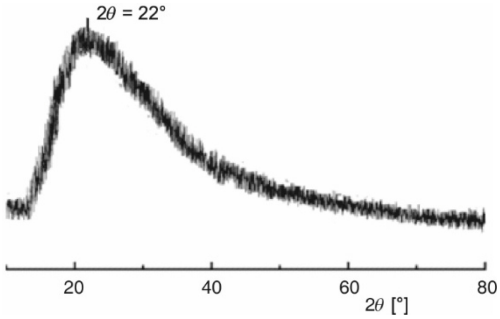

Figure 5. The XRD pattern of CD

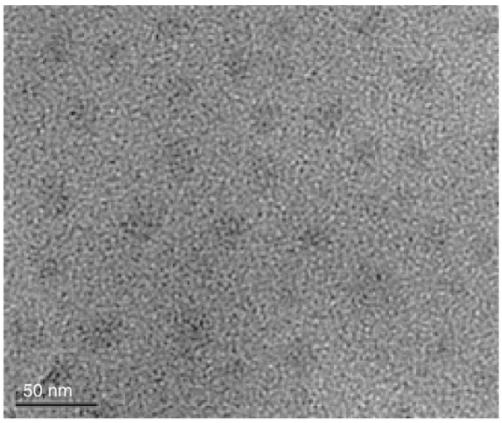

Figure 6. The TEM image of CD

Typical XRD pattern of CD is shown in fig. 5. The curve reflected a broad and strong diffraction peak centered at about 2θ = 22°, which was assigned to highly disordered (002) planes of graphitic carbon [16, 17]. The TEM was recorded to demonstrate the microstructures of CD, as shown in fig. 6. According to the TEM image, synthesized CD display spherical-like uniform shape and disperse well.

Conclusion

We systematically investigated the impact of operational parameters for synthesizing the CD using single factor experiment, including the synthesis temperature, time, the concentrations of citric acid monohydrate and urea. The PL intensity was adopted as the response value to evaluate significant factors effecting on their fluorescent performance. It is found that the best fluorescence performance was achieved when the synthesis temperature was kept of 190 °C, reaction time of 18 hours, citric acid monohydrate of 0.3 mol/L as well as urea of 1 mol/L. Notably, synthesis temperature obviously affected the property of CD. Under the optimized conditions, the synthesized materials exhibited noticeably superior luminescent property. In addition to the strong PL intensity, results from FTIR, XPS, as well as other tests demonstrated that the prepared CD consisted of carbon, oxygen, and hydrogen elements. The functional groups on the surface, *i. e.* hydroxyl, carboxyl and carbonyl, would provide great potential for novel applications in photocatalysis and energy conversion in the near future. The CD based nanofibers by bubble electrospinning or electrospinning [18-25] have received considerable attention due to their outstanding optical and catalytic properties, and the reaction equation can be easily solved by Taylor method [26].

Acknowledgment

We would like to acknowledge the financial support of the National Key R&D Program of China (No. 2017YFB0309100), Chinese Foundation Key projects of governmental cooperation in international scientific and technological innovation (No. 2016YFE0115700); the National Nature Science and Foundation of China (Grant No. 31470509), and the 111project (No. B17021). The authors would also like to thank Shiyanjia lab for their professional tests support.

References

[1] Kundu, A., *et al.,* Facile Approach to Synthesize Highly Fluorescent Multicolor Emissive Carbon Dots via Surface Functionalization for Cellular Imaging, *Journal of Colloid & Interface Science, 513* (2018), Mar., pp. 505-514

[2] Tuerhong, M., *et al.,* Review on Carbon Dots and Their Applications, *Chinese Journal of Analytical Chemistry, 45* (2017), 1, pp. 139-150
[3] Isnaeni, H. Y., Suliyanti, M. M., Concentration Effect on Optical Properties of Carbon Dots at Room Temperature, *Journal of Luminescence, 198* (2018), June, pp. 215-219
[4] Jaleel, J. A., Pramod, K., Artful and Multifaceted Applications of Carbon Dot in Biomedicine, *Journal of Controlled Release, 269* (2017), Jan., pp. 302-321
[5] Baker, S. N., Baker, G. A., Luminescent Carbon Nanodots: Emergent Nanolights, *Angew. Chem. Int. Ed, 49* (2010), 38, pp. 6726-6744
[6] Mishra, V., *et al.,* Carbon Dots: Emerging Theranostic Nanoarchitectures, *Drug Discovery Today, 23* (2018), 6, pp. 1219-1232
[7] Zhu, C., *et al.,* Carbon Dots Enhance the Stability of CdS for Visible-Light-Driven Overall Water Splitting, *Applied Catalysis B Environmental, 216* (2017), Nov., pp. 114-121
[8] Wang, N., *et al.,* Green Preparation of Carbon Dots with Papaya as Carbon Source for Effective Fluorescent Sensing of Iron (III) and Escherichia Coli, *Biosensors & Bioelectronics, 85* (2016), Nov., pp. 68-75
[9] Das, R., *et al.*, Carbon Quantum Dots from Natural Resource: A Review, *Materialstoday Chemistry, 8* (2018), June, pp. 96-109
[10] Wang J, *et al.*, Amphiphilic Egg-Derived Carbon Dots: Rapid Plasma Fabrication, Pyrolysis Process, and Multicolor Printing Patterns, *Angewandte Chemie International Edition, 51* (2012), 37, pp. 9297-9301
[11] Wu, Z. L., *et al.*, One-Pot Hydrothermal Synthesis of Highly Luminescent Nitrogen-Doped Amphoteric Carbon Dots for Bioimaging from Bombyx Mori Silk – Natural Proteins [J], *Journal of Materials Chemistry B, 22* (2013), 1, pp. 2868-2873
[12] Velusamy, J., *et al.,* Prominence of Fusion Temperature and Engineering Heteroatoms on Multifarious Emissive Shifts in Carbon Dots, *Journal of Colloid & Interface Science, 528* (2018), Oct., pp. 237-247
[13] Qu, S., *et al.,* Ratiometric Fluorescent Nanosensor Based on Water Soluble Carbon Nanodots with Multiple Sensing Capacities, *Nanoscale, 12* (2013), 5, pp. 5514-5518
[14] Hernandez-Rodriguez, M. A., *et al.,* Carbon Dots as Temperature Nanosensors in the Physiological Range, *Journal of Luminescence, 196* (2017), Apr., pp. 313-315
[15] Chen, Y., *et al.,* Facile Synthesis of Nitrogen and Sulfur Co-Doped Carbon Dots and Application for Fe (III) Ions Detection and Cell Imaging, *Sensors & Actuators B Chemical, 223* (2016), Feb., pp. 689-696
[16] Zhang, Y., *et al.*, Effect of Reaction Temperature on Structure and Fluorescence Properties of Nitrogen--Doped Carbon Dots [J], *Applied Surface Science, 387* (2016), Nov., pp. 1236-1246
[17] Krysmann, M. J., *et al.*, Formation Mechanism of Carbogenic Nanoparticles with Dual Photoluminescence Emission [J], *Journal of the American Chemical Society, 134* (2011), 2, pp. 747-750
[18] Chen, S., *et al.*, Carbon Dots/Fe_3O_4 Hybrid Nanofibers as Efficient Peroxidase Mimics for Sensitive Detection of H_2O_2 and Ascorbic Acid, *Inorg. Chem. Front., 4* (2017), 10, pp. 1621-1627
[19] Liu, L.-G., *et al.*, Solvent Evaporation In A Binary Solvent System For Controllable Fabrication Of Porous Fibers By Electrospinning, *Thermal Science, 21* (2017), 4, 1821-1825
[20] Liu, P., *et al.*, Geometrical Potential: an Explanation of Nanofibers Wettability, *Thermal Science, 22* (2018), 1A, pp. 33-38
[21] Yu, D. N., *et al.*, Snail-Based Nanofibers, *Mater. Lett., 220* (2018), June, pp. 5-7
[22] Liu, Y.-Q., *et al.*, Nanoscale Multi-Phase Flow and Its Application to Control Nanofiber Diameter, *Thermal Science, 22* (2018), 1A, pp. 43-46
[23] Tian, D., *et al.*, Self-Assembly of Macromolecules in a Long and Narrow Tube, *Thermal Science, 22* (2018), 4, pp. 1659-1664
[24] Liu, Y. Q., *et al.* Air Permeability of Nanofiber Membrane with Hierarchical Structure, *Thermal Science, 22* (2018), 4, pp. 1637-1643
[25] Zhao, L., *et al.*, Sudden Solvent Evaporation in Bubble Electrospinning for Fabrication of Unsmooth Nanofibers, *Thermal Science, 21* (2017), 4, pp. 1827-1832
[26] He, J.-H., Ji, F. Y., Taylor Series Solution for Lane-Emden Equation, *Journal of Mathematical Chemistry*, https://doi.org/10.1007/s10910-019-01048-7, 2019

Paper submitted: July 1, 2018
Paper revised: October 10, 2018
Paper accepted: October 10, 2018

© 2019 Society of Thermal Engineers of Serbia.
Published by the Vinča Institute of Nuclear Sciences, Belgrade, Serbia.
This is an open access article distributed under the CC BY-NC-ND 4.0 terms and conditions.